

A Diagnostic Model for Recognition of Recurrent Nasopharyngeal Carcinoma in Positron Emission Tomography/Computed Tomography (PET/CT) Based on Artificial Neural Networks

Fuk-hay Tang^{1*}, Elaine YN Pang¹ and Tao Chan²

¹Department of Health Technology and Informatics, The Hong Kong Polytechnic University, 11 Yuk Choi Rd, Hung Hom, Hong Kong

²Department of Diagnostic Radiology, University of Hong Kong, Pok Fu Lam, Hong Kong

Abstract

Purpose: Recurrent nasopharyngeal carcinoma after treatment can be difficult to recognize as there are overlapping imaging findings with post-radiotherapy changes. We have established an intelligent computerized system that differentiates recurrent carcinoma and normal condition using artificial neural network based on studies of Positron Emission Tomography/Computed Tomography with limited cases (n=16).

Method: Twenty-one validated radiological features were used as inputs for the neural network. The neural network was trained by leave-one-out cross-validation (LOOCV) method with 2 outputs.

Results: Our observer study indicated that when the radiologists are provided with the ANN output they make better decisions and there was significant improvement for junior radiologists after using neural network results (p<0.01).

Conclusion: This study demonstrated the feasibility of using artificial neural network for deciphering complex imaging pattern of recurrent nasopharyngeal carcinoma after treatment with limited case samples and improved the diagnostic accuracy of PET/CT for recurrent nasopharyngeal carcinoma.

Publication History:

Received: December 16, 2016

Accepted: February 06, 2017

Published: February 08, 2017

Keywords:

Artificial Neural Network, Recurrent Nasopharyngeal Carcinomas, Positron Emission Tomography, Computed Tomography, Radiologist's performance

Introduction

Nasopharyngeal Carcinoma (NPC) is one of most common malignant carcinoma affecting the Southern Chinese population [1]. For management of this tumor, radiotherapy (RT) or radiotherapy with concurrent chemotherapy (CCRT) is the mainstay treatment, whereas surgery is reserved for recurrent disease [2]. It has been reported that local recurrence of NPC occurs in approximately 15% to 54% in patients treated with RT or CCRT within 5 years [3]. In addition, there are variable changes in the nasopharyngeal tissues caused by radiotherapy, such as oedema, necrosis, and fibrotic changes, which complicate the picture [4,5]. The imaging signs due to overlapping features of recurrent NPC and radiotherapy treatment effects pose a diagnostic challenge for clinicians.

Artificial neural networks (ANNs) method has been proven to be a powerful tool for data classifications, pattern recognitions and predictions in medical imaging [6]. It has been used for various medical imaging applications such as lesion detection in SPECT, texture analysis in ultrasound, differential diagnosis of cerebral tumor on MRI [7] differential diagnosis of chest radiograph and high-resolution CT [8,9], and prediction of breast malignancy on mammograms [10]. ANNs have also been applied in tumor segmentation for NPC on MRI and development of NPC prognosis prediction model [11,12].

To the best of our knowledge, there has been no published report about the use of ANNs for evaluation of recurrent NPC using ¹⁸F-FDG PET/CT images. We also recognize that are small number of cases of tumour recurrence after radiotherapy treatment suitable for the training of ANNs. In this study, we proposed an ANNs scheme for limited samples that simulated the decision process of radiologist for recognizing recurrent NPC on ¹⁸F-FDG PET/CT images.

Materials and Method

Design of the Artificial Neural Network

Artificial neural networks (ANNs) method is a mathematical model or computational model simulating biological neural networks [13]. The setting of ANNs consists of Input Layer, Hidden Layer(s) and Output Layer:

Input Layer: for input neurons with activation, we took 21 radiological features as the input in the neural network.

Hidden Layer: activation function, σ , where w_{ij} and b_j was the weight from i th input neuron to j th hidden neuron.

Output Layer: neurons y_i was given by

$$y_i(\mathbf{x}) = \sum_{j=1}^N s_{ij} a_j(\mathbf{x}), i = \{1, 2, \dots, m\} \quad (1)$$

where s_{ij} was the weight from j th neuron in the i th hidden layer to the i th neuron of the output layer.

For detection of recurrent NPC using ¹⁸F-FDG PET/CT images, we designed the neural networks to mimic the neural capacity and processes for the decision process of experienced radiologists. Our design was composed of a three-layer, feed-forward ANNs with a back-propagation method using Levenberg-Marquardt algorithm for least square curve fitting based on the work by Hagan and Menhaj (14), implemented using Matlab ((The Mathworks Inc., Release 2010a). The feed forward network was designed with 21 input units for 21 radiological features identified during the pilot study

*Corresponding Author: Dr. Fuk-hay Tang, Department of Health Technology and Informatics, The Hong Kong Polytechnic University, Yuk Choi Road, Hung Hum Kowloon, Hong Kong, Tel: 853-34008564, Fax: 852-23624365; E-mail: fuk-hay.tang@connect.polyu.hk

Citation: Tang FH, Pang EY, Chan T (2017) A Diagnostic Model for Recognition of Recurrent Nasopharyngeal Carcinoma in Positron Emission Tomography/Computed Tomography (PET/CT) Based on Artificial Neural Networks. Int J Radiol Med Imag 3: 117. doi: <https://doi.org/10.15344/2456-446X/2017/117>

Copyright: © 2017 Tang et al. This is an open-access article distributed under the terms of the Creative Commons Attribution License, which permits unrestricted use, distribution, and reproduction in any medium, provided the original author and source are credited.

(see section 2.2.2), one-hidden layer and two output units corresponding to the likelihood of recurrent NPC and likelihood of normal findings. The ANNs were trained up to 500 iterations with an error goal of less than 0.1.

The training process comprised 9 normal cases and 7 abnormal cases. The feed-forward back propagation ANNs were trained using a round-robin (leave-one-out) method which was suitable for small training cases [15,16]. The idea of leave-one-out cross-validation (LOOCV) was that a single case was left out as the testing set, whilst the remaining 15 cases were used as the training data set. The procedure was repeated so that each of the 16 sets was used once as the testing set and the rest of the sets were used as the training sets.

Case selection and image acquisition

Case Selection

This was a retrospective study. The cases were firstly selected by the collaborative clinicians from the Radiology Information System in the imaging centre. The related images were retrieved from the Picture Archiving and Communications System and were anonymized to observe patient privacy. Ethics Committee approval was obtained by our institute.

It was because eligible cases of recurrent NPC after treatment were relative rare. As a result, during the period of our study, 16 NPC cases were selected; in which 7 cases were confirmed to have recurrent NPC clinically and all ¹⁸F-FDG PET/CT scan were preformed within 4 to 8 months after radiotherapy. Another 9 cases which were proven normal clinically were also obtained.

Establishment of the parameters for Recurrent NPC

A list of diagnostic features used for detecting recurrent NPC based on ¹⁸F-FDG PET/CT images were firstly obtained by the researchers in a pilot study. Three radiologists experienced in head and neck radiology (having 10 – 15 years of experience) were asked to identify the key diagnostic features related to recurrent NPC independently from the list. Only those diagnostic features agreed by all three radiologists in the list were used.

The ANN needed to be trained by the knowledge of experienced radiologists by giving the scores to the system. We invited other two radiologists with more than 10 years of experience to train the system. The experienced radiologists read all the images and gave their rating. One example of subjective ratings of one attending radiologist for recurrent NPC and normal case with the 21 diagnostic features is shown in table 1. The input data were scored by two experienced attending radiologists, which were subsequently normalized to between 0 to 10.

Observer Test

To evaluate the usefulness of our system, two radiology residents with one year of training in nuclear medicine and PET/CT were recruited in the observer test. They had no prior knowledge on the subjective ratings for radiological features described above. Receiver operating characteristic (ROC) studies was used to evaluate the performance of radiologists [7,8]. First, the observers were shown PET/CT images in the image workstation for initial rating of the confidence level of recurrent NPC (without ANNs output). The observers could

¹⁸ F-FDG PET/CT	Subjective Ratings (0 – 10)	
	Normal	Recurrent NPC
Size of dominant lesion	0	8
Lesion(s) at roof of the nasopharynx	0	7
Lesion(s) at retropharyngeal space	0	3
Lesion(s) at fossa of Rosenmueller	0	5
Mean SUV	3	7
Max SUV of the lesion(s)	2	7
Max SUV ratio of the lesion(s) to normal liver	3	7
Asymmetric ¹⁸ F-FDG uptake at LPR	2	2
Increase uptake of ¹⁸ F-FDG	3	8
Involvement of lymph node of roof of the nasopharynx	1	0
Involvement of lymph node of retropharyngeal space	1	0
Shape of lymph node	0	0
Max SUV of the lymph node	0	0
Size of the lymph node in submandibular region	0	0
Size of the lymph node in jugulodigastric region	1	0
Size of the lymph node in retropharyngeal region	1	0
Size of the lymph node at elsewhere	2	0
Wall thickening at LPR	3	3
Increased soft tissue density of fossa of Rosemuller	2	2
Central nodal necrosis	0	0
Distant metastases	0	0

Table 1: One Attending Radiologist's Subjective Ratings of normal and recurrent NPC case.

make their judgments according to their knowledge or using the 21 radiological features we used. Subsequently, ANNs outputs with calculated likelihood of recurrent NPC were displayed in the same workstation to the same observer who rated the confidence level a second time (with ANNs output). The observer's confidence level about the likelihood of recurrent NPC was represented using a continuous-rating scale with a line-checking method [7,8,14]. For the initial ratings, the observers used a blue ballpoint pen to mark their confidence levels along a 10-cm line. Ratings of "definitely no recurrent NPC", "indeterminate" and "definitely recurrent NPC" were marked above the left end, center and right end of the line respectively. If the second ratings were different from the initial ones, the observers used a red ballpoint pen to mark their confidence levels along the same line. For data analysis, the confidence level was scored by measuring the distance from the left end of the line to the marked point and converting the measurement to a scale from 0 to 100.

Data Analysis

The performances of the ANNs, radiologists' diagnostic performance with and without ANNs and diagnostic model were evaluated using ROC analysis. Binormal ROC curves for diagnosing recurrent NPC were estimated using ROCKIT 0.9B developed by

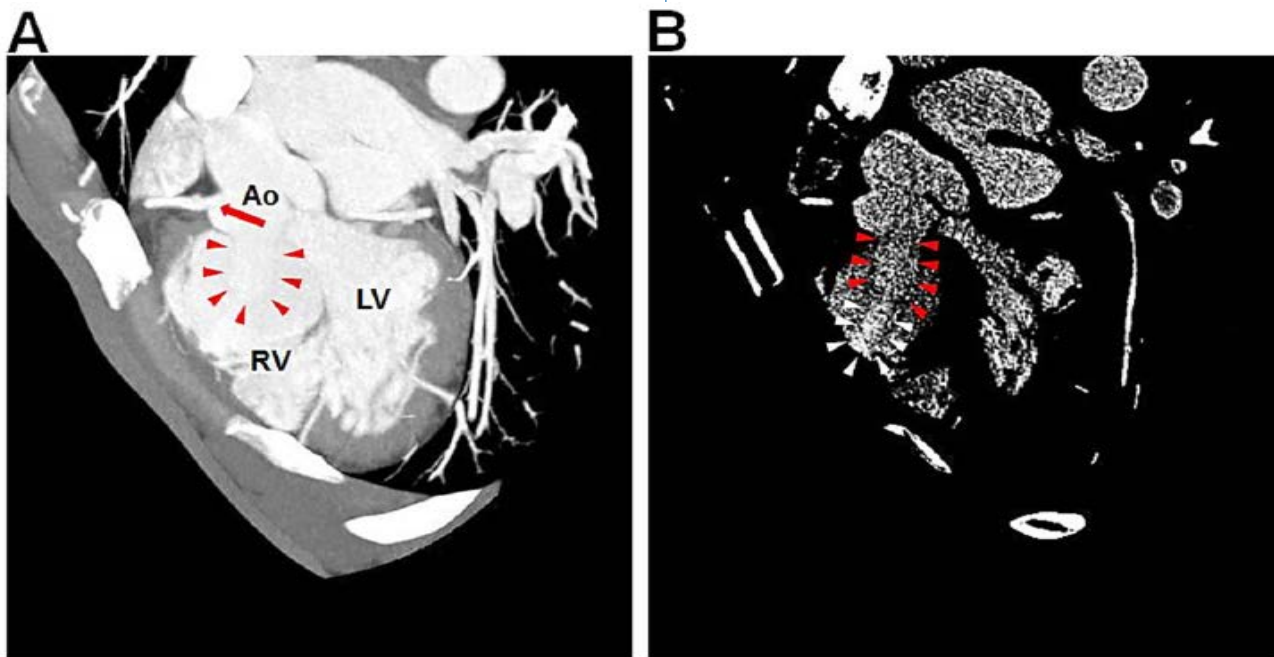


Figure 3: Cardiac computed tomography. Cardiac computed tomography shows ring-like structure originating from the right coronary sinus of the aortic valve protruding to the right ventricle (red arrow heads) (A and B) with extravasation of the radiocontrast agent (white arrow heads) (B). The right coronary ostium is not involved by aneurysm (red arrow) (A). Ao, aorta; RV, right ventricle; LV, left ventricle.

those of aforementioned cardiac CT. TEE revealed a protruding aneurysmal sac with shunting from the right coronary sinus to RV (Figure 4 and Video 3). Invasive cardiac catheterization was not performed. Surgical findings confirmed a large aneurysm with a defect at right coronary sinus of the AV. There was no

other combined cardiac pathology. Resection of the aneurysmal sac and repair of the aortic root using an autologous pericardial patch was performed. After surgery, TTE no longer showed abnormal shunt flow at the aortic root except minimal valvular regurgitation of the AV (Figure 5 and Video 4). She has been doing well without chest symptoms after surgery.

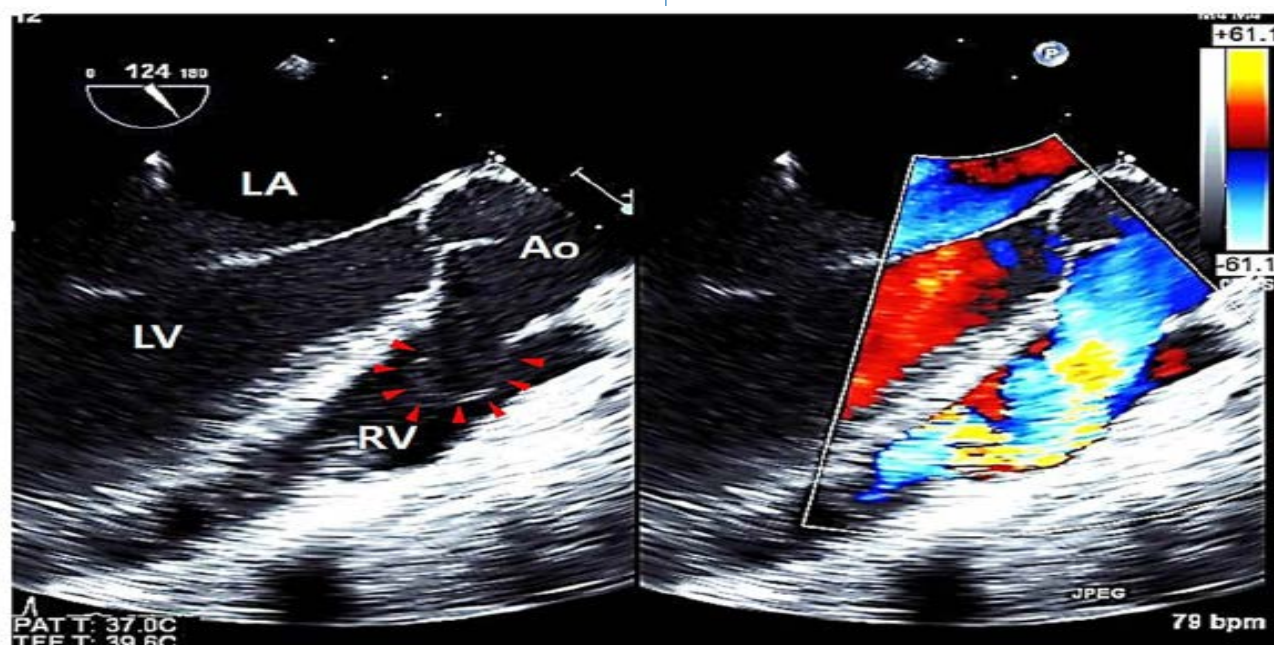


Figure 4: Transesophageal echocardiography. Transesophageal echocardiography shows a protruding aneurysmal sac (red arrow heads) with shunting from the right coronary sinus to the right ventricle. LA: left atrium; LV, left ventricle; Ao, aorta; RV, right ventricle.

the Department of Radiology of the University of Chicago [17]. Az value representing the area under the ROC curve was calculated. The statistical significance of differences between ROC curves were determined by applying chi-square test for paired data to specific area under the curve (AUC, or Az value).

Results

The sensitivity of correct classification of the ANNs following training for predicting recurrent NPC was 79% and the specificity is 100%. The Az value of the ANN alone was 0.921, indicating a high performance (Figure 1). Table 2 shows the Az value with and without ANN output for the two radiology residents. The performance for both residents improved significantly when ANN output was used ($p < 0.01$). The overall performance of the two observers was illustrated by the average ROC curves in Figure 2. The average Az value increased to a statistically significant level from 0.523 without ANN output to 0.805 with ANN output ($p < 0.0001$). However, the average Az value of observers with ANN output was still lower than for the ANN alone.

Discussion

We have proposed an intelligent system for differentiating recurrent NPC from normal features by simulating the decision process of radiologists using artificial neural networks.

For the construction of the ANNs in this study, 21 radiological features of recurrent NPC on ¹⁸F-FDG PET/CT images were selected and translated as scores for data input for ANNs. We found that the ANNs showed a high performance (Az = 0.921). This finding was comparable to the performance of ANNs constructed in other studies which reported Az values from 0.940 to 0.977 [7, 8, 15]. It indicates that the ANNs can recognize the complex interactions and patterns on radiological features as input data and thereby learn the relationship between the input data and output data, which are likelihood of recurrent NPC and likelihood of normal finding.

In our observer test, for the two participating residents with one year of experience in interpretation of ¹⁸F-FDG PET/CT images, there was significant improvement in diagnostic performance on the evaluation of recurrent NPC using PET/CT images with ANN output ($p < 0.0001$) (Figure 2). This finding was in accordance with several previous studies and indicated that ANNs may be helpful for readers with limited clinical experience [7, 8, 15]. It could be reasonably suggested that the ANN would help clinicians with less clinical experience in recognition of significant PET/CT features of recurrent NPC by alerting them to reconsider certain diagnostic features through careful interpretation of radiological features, arriving at a correct diagnosis (Table 2). On the other hand, while our result suggested that ANN was helpful for readers with limited clinical experience, we believed that further study is required to determine the usefulness of ANN in the evaluation of recurrent NPC based on PET/CT images for radiologists with different levels of experience.

Observer	Without ANN	With ANN	p
A	0.36	0.695	<0.001
B	0.616	0.891	<0.01

Table 2: Comparison of Az Values Without and With ANN Output

In this study, the ANN was developed with 21 radiological features without any clinical parameters as input data. To further enhance the practical application of this diagnostic model in the future, some useful clinical data, such as infection of Epstein-Barr virus (EBV), stage of primary NPC and dietary habits, could be included as input data. Higher diagnostic performance of the ANNs obtained with a combination of clinical parameters and radiological findings as input data was reported by previous studies [15, 18]. It is therefore expected that with the combination of clinical parameters and radiological features as input data, the performance of the diagnostic model can be further enhanced for practical use. Although the number of cases for our study was quite limited, our attempt to construct a computer-aided diagnostic scheme using ANNs that was proven to be useful.

Conclusion

ANNs showed a high performance in evaluation of recurrent NPC based on ¹⁸F-FDG PET/CT images. Its outputs can provide a second opinion to improve the accuracy and efficiency for clinicians in diagnosis. In addition, we have established a diagnostic model based on CAD for evaluation of recurrent NPC based on ¹⁸F-FDG PET/CT images.

Competing Interests

The authors have no competing interests with the work presented in this manuscript.

References

- Ahuja A, Evans R, King A, van Hasselt C (2003) *Imaging of Head and Neck Cancer*. London: Greenwich Medical.
- Brennan B (2006) *Nasopharyngeal Carcinoma*. *Orphanet Journal of Rare Diseases* 1: 23-28
- Li PY, Zhuang HM, Mozley PD, Denittis AI, Yeh D, et al. (2001) Evaluation of Recurrent Squamous Cell Carcinoma of the Head and Neck with FDG Positron Emission Tomography. *Clin Nucl Med* 26: 131-135.
- Chen YK, Su CT, Chi KH, Cheng RH, Wang SC, et al. (2007) Utility of ¹⁸F-FDG PET/CT Uptake Patterns in Waldeyer's Ring for Differentiating Benign from Malignant Lesions in Lateral Pharyngeal Recess of Nasopharynx. *J Nucl Med* 48: 8-14.
- Yen RF, Hung RL, Pan MH, Wang YH, Huang KM, et al. (2003) ¹⁸-Fluoro-2-Deoxyglucose Positron Emission Tomography in Detecting Residual/ Recurrent Nasopharyngeal Carcinomas and Comparison with Magnetic Resonance Imaging. *Cancer* 98: 283-287.
- Burke HB (1997) Evaluating Artificial Neural Network for Medical Applications. *Artificial Networks* 4: 2494-2496.
- Yamashita K, Yoshiura T, Arimura H, Mihara F, Noguchi A, et al. (2008) Performance Evaluation of Radiologists with Artificial Neural Network for Differential Diagnosis of Intra-Axial Cerebral Tumors on MR Images. *AJNR Am J Neuroradiol* 29: 1153-1158.
- Nie Y, Li Q, Li F, Pu Y, Appelbaum D, et al. (2006) Integrating PET and CT Information to Improve Diagnostic Accuracy for Lung Nodules: A Semiautomatic Computer-Aid Method. *The Journal of Nuclear Medicine* 47: 1075-1080.
- Matsuki Y, Nakamura K, Watanabe H, Aoki T, Nakata H, et al. (2002) Usefulness of an Artificial Neural Network for Differentiating Benign from Malignant Pulmonary Nodules on High-Resolution CT: Evaluation with Receiver Operating Characteristic Analysis. *AJR Am J Roentgenol* 178: 657-663.
- Floyd CE, Lo JY, Yun AJ, Sullivan DC, Kornguth PJ (1994) Prediction of Breast Cancer Malignancy Using an Artificial Neural Network. *Cancer* 74: 2944-2948.

11. Zhou J, Chong V, Lim TK, Huang J, et al. (2002) MRI Tumor Segmentation for Nasopharyngeal Carcinoma Using Knowledge-based Fuzzy Clustering. *International Journal of Information Technology* 8: 36-45.
12. Kareem SA, Baba S, Zubairi YZ, Prasad U, Ibrahim M, et al. (2002) Prognostic System for NPC: A Comparison of the Multi Layer Perception Model and the Recurrent Model. *Neural Information Processing* 1: 271-275.
13. Lisboa PJG, Ifeachor EC, Szczepaniak PS (2000) *Artificial neural networks in biomedicine*. Springer (London).
14. Hagan M, Menhaj M (1994) Training Feedforward Networks with the Marquardt Algorithm. *IEEE Transactions on Neural Networks* 5: 989-993.
15. Fukushima A, Ashizawa K, Yamaguchi T (2004) Application of an Artificial Neural Network to High-Resolution CT: Usefulness in Differential Diagnosis of Diffuse Lung Disease. *AJR Am J Roentgenol* 183: 297-305.
16. Näppi JJ, Frimmel H, Dachman AH, Yoshida H (2004) Computerized detection of colorectal masses in CT colonography based on fuzzy merging and wall-thickening analysis. *Med Phys* 31:860-872.
17. Metz CE (2006) Receiver operating characteristic (ROC) analysis: a tool for quantitative evaluation of observer performance and imaging systems. *J Am Coll Radiol* 3: 413-422.
18. Grenier P, Chevret S, Beigelman C, Brauner MW, Chastang C, et al. (1994) Chronic Diffuse Infiltrative Lung Disease: Determination of the Diagnostic Value of Clinical Data, Chest Radiology, CT and Bayesian Analysis. *Radiology* 191: 383-339.